Reviews in Mineralogy & Geochemistry
Vol. 57, pp. 291-305, 2005

A Short Outline of the Tunnel Oxides

Marco Pasero
Dipartimento di Scienze della Terra
Università di Pisa
Via S. Maria 53
I-56126 Pisa, Italy
pasero@dst.unipi.it

INTRODUCTION

Within the large and comprehensive group of oxide minerals (class 4 in the Strunz classification; Strunz and Nickel 2001), the most relevant subgroup in the frame of microporous materials is that of the so-called "tunnel oxides." This rather generic term historically refers to a number of minerals which, from a chemical point of view, are (mainly) manganese oxides. In nature manganese occurs in three different oxidation states—Mn^{2+}, Mn^{3+} and Mn^{4+}—with the latter being the dominant form in tunnel oxides. Tetravalent manganese typically has octahedral coordination, and using only $[Mn^{4+}O_6]$ building modules linked together *via* corner- and edge-sharing it is feasible to construct many framework structures. Besides, a set of titanate minerals display the same feature, as might be expected due to the similar crystal-chemical behaviour of Mn^{4+} and Ti^{4+} cations. Therefore, this note is devoted to describing the structural principles and arrangements of minerals—and a number of synthetic compounds as well—in which the dominant cations are Mn^{4+} and Ti^{4+}.

Starting from the basic formula of manganese dioxide, $Mn^{4+}O_2$, incorporation of mono- and divalent cations (primarily alkali and alkali earths) within the tunnels of the structures, can be accommodated by partial reduction of manganese. Until recently, there was a considerable uncertainty and lively debate (e.g., Burns et al. 1983; Burns et al. 1985; Giovanoli 1985) concerning the valence of the reduced species and whether Mn^{2+} or Mn^{3+} was present. It is now commonly accepted on the basis of several high-quality structural studies that Mn^{3+} replaces Mn^{4+}. In titaniferous phases, charge balance accompanying the inclusion of tunnel cations is not adjusted by reduction to Ti^{3+}, but through incorporation of Fe^{3+}, V^{3+} or Cr^{3+} substituting for Ti^{4+}. The generic substitutions can be summarized in the generic formula:

$$A^{+}_{x}(M^{3+}_{x}M^{4+}_{1-x})O_2 \text{ or } A^{2+}_{x}(M^{3+}_{2x}M^{4+}_{1-2x})O_2$$

where $A = Na^{+}$, K^{+}, Rb^{+}, Mg^{2+}, Ba^{2+}, Pb^{2+}; $M^{3+} = Mn$, Fe, V, Cr, Al; and $M^{4+} = Mn$ or Ti. Water molecules can also enter the tunnels.

BASIC STRUCTURAL FEATURES

In all these compounds $[Mn^{4+}O_6]$ or $[Ti^{4+}O_6]$ octahedra are arranged in edge-sharing columns, which in turn link together, again by edge-sharing, to construct ribbons, with widths potentially ranging from 1 to ∞. Cross-linking by corner-sharing of columns or ribbons in near perpendicular directions, gives rise to a number of different tunnel structures that may be square or rectangular, depending on the dimensions of the ribbons. The ideal topological symmetry of the frameworks is either tetragonal (for structures with the same dimensionality in the two directions, e.g., 1×1, 2×2,…) or orthorhombic. In most cases the real symmetry is lower, the

1529-6466/05/0057-0009$05.00 DOI: 10.2138/rmg.2005.57.9

deviation arising from minor distortions of the framework and/or ordered distributions of cations. In a number of examples substitution of M^{4+} by trivalent (or even divalent) cations can be balanced by the insertion of large mono- or divalent cations within the tunnels. Typically, the unit cell axis along the direction in which the octahedral columns or ribbons run is 2.8–2.9 Å, corresponding to a single octahedron repeat. Clearly, the two unit cell parameters in the orthogonal plane depend on the width of the ribbons. What follows is a short outline of all the known tunnel structure-types belonging to this group in order of increasing complexity. Throughout the paper we will speak of "tunnels" to conform to the historical naming of those structures and the long-time custom, although we are aware that, according to the IUPAC recommendation, it should be more correct to denote them as "channels" (McCusker 2005).

1×1 tunnels

The basic 1 × 1 structure is adopted by the simplest and most common form of manganese dioxide, β-MnO_2 or pyrolusite. This mineral (tetragonal, $P4_2/mnm$, $a=4.3983$, $c=2.8730$ Å; Baur 1976) is isostructural with rutile, the commonest polymorph of TiO_2. Many other $M^{4+}O_2$ compounds isostructural with pyrolusite and rutile are known, including cassiterite ($M=Sn^{4+}$), plattnerite ($M=Pb^{4+}$) and argutite ($M=Ge^{4+}$), as well as stishovite, the high pressure polymorph of silica. According to De Wolff (1959), another form of pyrolusite exists—it has orthorhombic symmetry and is thought to be an alteration product of manganite, γ-MnO(OH). Rietveld refinement of orthorhombic pyrolusite has been completed (Yoshino et al. 1992, 1993) and showed that Mn^{4+} is partially substituted by Mn^{3+} (with charge compensation by H^+) in keeping with the general formula $Mn^{4+}_{1-x}Mn^{3+}_{x}O_{2-x}(OH)_x$. According to Kikuchi et al. (1994) only pure pyrolusite ($x=0$ in the above chemical formula) has tetragonal symmetry, with the following unit cell parameters derived by means of lattice energy calculations: $a=4.4424$, $c=2.8359$ Å (tetragonal, $x=0$); $a=4.4609$, $b=4.6113$, $c=2.7461$ Å (orthorhombic, $x=0.1$). The pure Mn^{3+}end member ($x=1$) is manganite *stricto sensu*, γ-MnO(OH), whose crystal structure has been studied by Dachs (1963). In pyrolusite and related phases the channels of the 1 × 1 framework are too small for incorporation of large cations.

1×2 tunnels

The crystal structure of ramsdellite was first determined by Byström (1949) as orthorhombic, space group *Pbnm*, $a=4.533$, $b=9.27$, $c=2.866$ Å. More recently, refinements of natural (Miura et al. 1990) and synthetic γ-MnO_2 (Fong et al. 1994) were presented that confirmed the essential features of the earlier work.

The hydroxide form of ramsdellite in which $Mn^{4+} \rightarrow Mn^{3+} + H^+$ is groutite, $Mn^{3+}O(OH)$, which corresponds to synthetic α-MnO(OH), and initially reported to be isostructural with ramsdellite (Dent Glasser and Ingram 1968). Lately, the structural relationship between ramsdellite and groutite has been examined in detail by Post et al. (2001), who discovered that most natural ramsdellites contain domains of a second isostructural phase with larger cell parameters, intermediate between those of ramsdellite and groutite. The intermediate phase, called "groutellite," has a longer <Mn–O> distance and increased Jahn-Teller distortion than pure ramsdellite, indicating a partial substitution of Mn^{4+} by Mn^{3+}. The crystal structure of "groutellite" has been refined by Post and Heaney (2004).

1×3 tunnels

Presently, no 1 × 3 tunnel oxide has been reported among minerals or synthetic compounds although unit cell scale occurrences are known in nsutite. This mineral which is polymorphic with synthetic γ-MnO_2 was defined as a new mineral species by Zwicker et al. (1962) and is named after the type locality (Nsuta, Ghana). Comprehensive high resolution transmission electron microscopy (HRTEM) of nsutite from the type locality and Piedras Negras, Mexico

(Turner and Buseck 1983) revealed at both occurrences a fine-scale intergrowth of domains of pyrolusite and ramsdellite, or more complex and faulted sequences. As such, maybe nsutite should not deserve the status of mineral, although it is still considered a valid species (Gaines et al. 1997). In the HRTEM image (Fig. 1) 1×3 cavities alternate with 1×2 cavities giving rise to a complex superstructure, in a narrow (*ca.* 100 Å wide) domain. So, while 1×3 cavities may be formed, it could not be energetically favorable for them to exist as extended structures. In this respect, however, it is worth noting that the relative stability of the various polymorphs of manganese dioxide seems little affected by their "openness" (Fritsch et al. 1997).

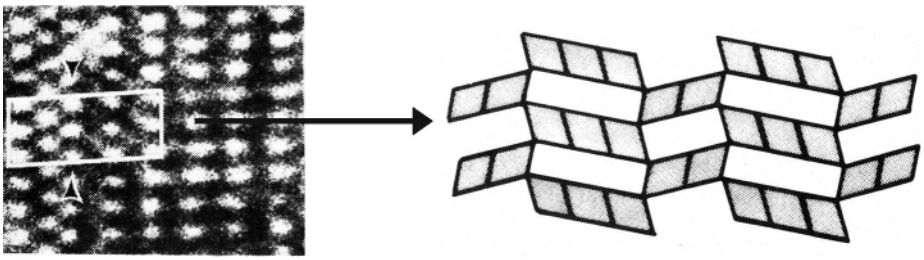

Figure 1. On the left side, HRTEM photo of nsutite from Piedra Negras, Mexico, showing a regular alternation of 1×2 and 1×3 tunnels. The structural arrangement of ribbons in the region within the B box is sketched on the right side [Used by permission of Nature Publishing Group, from Turner and Buseck (1983), Nature, Vol. 304, Fig. 2, p. 144].

2×2 tunnels

The 2×2 tunnel structure is most common, being displayed in several minerals and synthetic compounds. The best known example is hollandite which can be represented by the simplified formula $BaMn^{4+}{}_6Mn^{3+}{}_2(O,OH)_{16}$, although wide compositional variability has been reported involving substitutions of Mn^{3+} by Fe^{3+} or Al^{3+}. The crystal structure corresponds to the α-MnO_2 type and was solved by Byström and Byström (1950, 1951) from Weissenberg films. While the original description was made in the *I*4/*m* space group, i.e., assuming the ideal topological symmetry, a more precise refinement (Post et al. 1982) showed the true structure to be monoclinic *I*2/*m*, with $a=10.026$, $b=2.8782$, $c=9.729$ Å, $\beta=91.03°$.

Cryptomelane is analogous to hollandite, the difference lying only in the A cation where potassium replaces barium. Its structure has been refined by Post et al. (1982) in the *I*2/*m* space group with $a=9.956$, $b=2.8705$, $c=9.706$ Å, $\beta=90.95°$. A monoclinic-tetragonal transformation of cryptomelane at high temperature has been observed by Kudo et al. (1990). Moreover, Vicat et al. (1986) refined, at room temperature, the structure of a synthetic cryptomelane in the tetragonal space group *I*4/*m*, with $a=9.866$, $c=2.872$ Å.

Coronadite is the plumbous analogue of hollandite and cryptomelane with its crystal structure refined (Post and Bish 1989) using two different samples (from Bou Tazzoult, Morocco and from Broken Hill, Australia) in the space group *I*2/*m*, with $a=9.938$, $b=2.8678$, $c=9.834$ Å, $\beta=90.39°$ (unit cell from the Moroccan sample).

Among titanium oxides, priderite displays the 2×2 topology. The simplified chemical formula of priderite is $(K,Ba)_{1-2}(Ti^{4+},Fe^{3+})_8O_{16}$. However, in this case the symmetry is tetragonal rather than monoclinic as proven by two independent and near simultaneous studies (Sinclair and McLaughlin 1982; Post et al. 1982), the latter authors determination pointing to *I*4/*m*, $a=10.139$, $c=2.9664$ Å. Priderite with octahedral Fe^{2+} in place of Fe^{3+} has been synthesized at high pressure and is thought to occur in the mantle (Foley et al. 1994)

The crystal structures of four other titanate minerals belonging to the 2×2 family are reported. The crystal structure of mannardite, ideally $BaTi_6V_2O_{16}\cdot H_2O$, was solved by Szymański (1986) ($I4_1/a$, with $a=14.357$, $c=5.908$ Å), and although topologically identical to hollandite, has been described in a larger cell, with c parameter multiplied by 2 and a parameter multiplied by $\sqrt{2}$ presumably as a result of intertunnel ordering of barium. A similar behavior was also recorded on a sample of mannardite from Kyrgyzstan, which gave a quintuple c parameter ($a=10.071$, $c=14.810$ Å; Bolotina et al. 1992). In the closely related mineral ankangite, a supercell with a c parameter 14 times as large as the subcell was reported (Wu and Li 1990; Shi et al. 1991). The crystal structure of redledgeite $BaTi_6Cr_2O_{16}\cdot H_2O$ was solved by Gatehouse et al. (1986) in the monoclinic space group $I2/m$, and then redetermined by Foley et al. (1997) in the tetragonal space group $I4/m$ (with $a=10.150$, $c=2.9520$ Å). The latter authors also proposed a plausible occupancy model for Ba cations within the tunnels, in which Ba-Ba distances shorter than 4.1 Å were avoided. According to the proposed model, the general chemical formula of redledgeite can be written $Ba_x(M^{3+}_{2x}Ti^{4+}_{8-2x})O_{16}$, where $x \leq 1.33$. Henrymeyerite is a Ba-Fe titanate with ideal chemical formula $BaFe^{2+}Ti_7O_{16}$ found in the Kovdor complex, Kola peninsula, Russia (Mitchell et al. 2000). Henrymeyerite, a rare example where the tetravalent framework cation is replaced by a divalent species, is tetragonal ($I4/m$, $a=10.219$, $c=2.963$ Å). A phase with the same composition was also synthesized.

The structural distortion which lowers the symmetry from tetragonal to monoclinic in hollandite-type minerals has been discussed by Post et al. (1982) and Zhang and Burnham (1994), who studied the dependence of the symmetry on the radii of A (tunnel) and B (octahedral) cations.

A number of other minerals have been described, whose structures remain unknown, but which are likely to have the same 2×2 topology. Manjiroite is the sodium-rich analogue of hollandite with formula $(Na,K)(Mn^{4+},Mn^{3+})_8O_{16}$, and with unit cell parameters refined in the tetragonal space group $I4/m$ to $a=9.916$, $c=2.864$ Å (Nambu and Tanida 1967). Like priderite, it is possible that manjiroite may display the ideal topological symmetry. On the other hand strontiomelane, the Sr-dominant analogue of cryptomelane, has the ideal chemical formula $SrMn^{4+}_6Mn^{3+}_2O_{16}$ and $P2_1/n$ symmetry, which is a subgroup of $I2/m$, the space group of the majority of the hollandite-group minerals. The lowering of symmetry in strontiomelane is related to the doubling of the b axis (unit cell: $a=10.00$, $b=5.758$, $c=9.88$ Å, $\beta=90.64°$; Meisser et al. 1999).

A lead titanate analogue of coronadite has yet to be found, although plumbous henrymeyerite was recently described from the Murun alkaline complex, Yakutia, Russia (Reguir et al. 2003). In that sample, Pb reaches 0.45 apfu although not enough to be considered a new mineral species. Another feature of henrymeyerite from this latter occurrence, besides the solid-solution between Ba and Pb end members, is that iron is mainly in its trivalent state and its chemical formula may be best described as $(Ba,Pb)(Fe^{3+}_2Ti_6)O_{16}$. Moreover, Reguir et al. (2003) also synthesized the ideal Pb end member with composition $Pb(Fe^{3+}_2Ti_6)O_{16}$, and a number of intermediate compounds. For one of them, with composition $(Ba_{0.58}Pb_{0.51})_{\Sigma 1.09}(Ti,Fe)_8O_{16}$ a Rietveld refinement was also carried out.

Thus, the 2×2 tunnel structure allows considerable flexibility in chemical composition, as a result not only of tunnel cation exchange, but also of octahedral framework replacements. Indeed, besides the manganate and titanate minerals, many synthetic compounds are known to assume this framework topology. In early work, Bayer and Hoffman (1966) synthesized several compounds with the general formulae $A_2(Ti^{4+}_6M^{3+}_2)O_{16}$ (where A=K, Rb and M^{3+}=Al, Ti, Cr, Fe, Ga), or $A_2(Ti^{4+}_7M^{2+})O_{16}$ (where A=K, Rb and M^{2+}=Mg, Co, Ni, Cu, Zn). A compound with ideal chemical formula $BaAl_2Ti_6O_{16}$ was studied by Sinclair et al. (1980).

High pressure transformations of a number of alkali aluminosilicate and aluminogermanates ($KAlSi_3O_8$, $KAlGe_3O_8$, $NaAlGe_3O_8$, $RbAlGe_3O_8$) which assume the hollandite structure have been discussed by Ringwood et al (1967b). Moreover, Ringwood et al (1967a) described in detail a high-pressure (9 GPa) hollandite-type modification of K-feldspar ($KAlSi_3O_8$) with octahedrally coordinated Si^{4+}. This represented, at that time, the second known occurrence of a compound with $^{[6]}Si$ after stishovite. The crystal structure of high-pressure $KAlSi_3O_8$ was refined by powder XRD (Yamada et al. 1984) and single-crystal methods (Zhang et al. 1993). Since then, other very high pressure aluminosilicate phases were reported with the hollandite-type structure, e.g., $(Ca_{0.5}Mg_{0.5})Al_2Si_2O_8$ at 50 GPa (Madon et al. 1989), or $Pb_{0.8}Al_{1.6}Si_{2.4}O_8$ at 16.5 GPa (Downs et al. 1995).

2×3 tunnels

Romanechite, $Ba(Mn^{4+},Mn^{3+})_5O_{10}\cdot H_2O$, has been known since the earliest days of mineralogy and it is often referred to as psilomelane. The latter name is now discredited, being used for any poorly defined hard black manganese oxides. The crystal structure of romanechite was solved by Wadsley (1953) and re-determined by Turner and Post (1988). Romanechite is monoclinic, *C*2/*m*, $a=13.929$, $b=2.8459$, $c=9.678$ Å, $\beta=92.39°$. Structurally, it is a manganese oxide with 2x3 tunnels. Tunnels are occupied by barium cations and water molecules; the latter take part in the coordination polyhedra of barium, completed by oxygen atoms belonging to the walls of the tunnel. Turner and Post (1988) also refined a superstructure of romanechite, having a triple *b* axis, as a result of ordering of Ba and H_2O along the tunnel length; 3*b* (and, besides, 2*a*) multiples were already detected by Chukhrov et al. (1983) by electron diffraction, and were ascribed to the same phenomenon, although this not supported by HRTEM.

A HRTEM study carried out by Turner and Buseck (1979) on samples from Rattlesnake mine, Socorro Co., New Mexico, USA showed the conspicuous occurrence of romanechite-hollandite intergrowths; besides, some unusual insulated tunnels (2×4 and 2×7) were also observed. Recently, a compound structurally related to romanechite with $Na+H_2O$ within the 2×3 tunnels has been synthesized by Shen et al. (2004).

2×4 and 2×5 tunnels

Even larger tunnels have been observed outside the mineral kingdom. 2×4 tunnels were found in compounds with ideal formula close to $Rb_{0.25}(Mn^{4+},Mn^{3+})O_2$ (Rziha et al. 1996) and $Na_{0.33}(Mn^{4+},Mn^{3+})O_2\cdot xH_2O$ (Xia et al. 2001; Liu and Ooi 2003). Another synthetic compound with composition $Rb_{0.27}(Mn^{4+},Mn^{3+})O_2$ is based upon 2×5 tunnels (Tamada and Yamamoto 1986). This suggests that the dimensions of the tunnels are related to the extent of the substitution $Mn^{4+}\rightarrow Mn^{3+}+A^+$ and that the ionic radius of the A^+ cation can play some role in the formation of large tunnels. It is reasonable to expect that more complex tunnel structures can be tailored in controlled chemical environments.

3×3 tunnels

The first insight that todorokite displays a tunnel structure based on a new kind of net, 3×3 octahedra wide, was gained through electron microscopy. Turner and Buseck (1981) proposed this new structural model for todorokite, today well accepted, by means of a careful HRTEM study carried out on samples from Chargo Redondo (Cuba) and Bombay (India). Besides unravelling the basic structural features of the mineral, that study also revealed that at the atomic scale, tunnels with different dimensions may be intergrown. In particular, locally, 3×4, 3×5, 3×6, and 3×7 tunnels were observed. Normally, such tunnels are isolated within dominant 3×3 tunnels, with few exceptions (for instance, a sequence of three 3×4 tunnels is shown). Faulted sequences develop along only one direction: in todorokite, the walls along the other direction are invariably 3 octahedra wide. Chukhrov et al. (1980, 1985) also recorded a number of selected area electron diffraction patterns in todorokites from Bakal (Russia),

Sterling Hill (USA) and Takhta-Karacha (Central Asia) that were interpreted as arising from the occurrence of 3×9 wide tunnels. Although this hypothesis is supported by SAED, rather than high resolution lattice imaging, it is strong evidence of substantial inhomogeneity at the unit cell scale. A typical feature of todorokite, revealed by both optical and electron microscopy, was the occurrence of trilling (three twin individuals at 120°) a feature also observed in a synthetic compound with the same topology as todorokite (Golden et al. 1986). Finally, the crystal structure of todorokite was solved by Post and Bish (1988) by powder XRD since the mineral typically occurs as fine-grained crystals. A more precise Rietveld refinement using synchrotron radiation was presented recently (Post et al. 2003b).

3×4 tunnels

The prototype woodruffite occurs at Sterling Hill, NJ, USA (Frondel 1953) and was earlier considered as a Zn-rich variety of todorokite. At the type locality, woodruffite invariably occurs as fine-grained masses, which are unsuitable for single-crystal XRD analysis. Another occurrence (Mapimi, Durango, Mexico) gave tiny, needle-like crystals that proved suitable for investigation using a high intensity synchrotron X-ray source (Post et al. 2003a) that lead to a structure solution which confirmed an opening of 3×4 octahedral units, the largest so far described in either natural or synthetic systems.

A comprehensive list of known natural and synthetic tunnel oxides, including the basic chemical formula and the unit cell parameters, is reported in Table 1.

STRUCTURAL DETAILS

Octahedral distortion

By considering the complete set of structural data for the tunnel oxides, some recurring features concerning octahedral distortion can be rationalised. For testing purposes, only good-quality structural data for each type of tunnel structure were selected, and the octahedral distortion in each independent octahedron was calculated using the well-known equation $\Delta = 1/6\ \Sigma[(R_i - R)/R]^2$, where R_i is an individual M–O bond length and R is the average bond length in each octahedron. The results are presented in Table 2.

Overall, it can be seen that octahedral distortion is related to increasing structural complexity, the lowest distortion occurring in the 1×1 structure and increasing for larger tunnels. In pyrolusite, the [MnO_6] octahedron shows moderate distortion, with four equatorial Mn-O bonds slightly shorter (by 0.015 Å on average) than two apical Mn–O bonds. In ramsdellite, with a 1×2 tunnel, Mn–O distances are in the range 1.81–1.97 Å and octahedral distortion is greater than in pyrolusite. Such a trend is confirmed by the structures with larger tunnels.

The relationship between the dimensions of the tunnels and the degree of distortion can be related to the greater extent, in structures with large tunnels, of the substitution $^{VI}M^{4+} = {}^{VI}M^{3+} + A^{+}$ (or $^{VI}M^{4+} = 2\,{}^{VI}M^{3+} + A^{2+}$). The distortion is more evident when the dominant trivalent cation is Mn^{3+}, which is known to display Jahn-Teller effects. In addition, in tunnel oxides with a square outline (e.g., 2×2, 3×3) distortion is less pronounced than expected. It is also noted that in cases of wide ribbons, the distortion is most evident in external octahedra due to the tendency for trivalent cations to concentrate in those sites.

Extra-framework positions

The capacity of the tunnel oxides to incorporate larger cations is obviously related to channel dimension, and consequently the 1×1 tunnel structures (pyrolusite- and rutile-type) circumscribe an interstitial that is too small to accommodate a cation. Similarly, the 1×2 the tunnels do not show significant cation incorporation, although Potter and Rossman (1979)

Table 1. A selection of unit cell parameters for tunnel oxide compounds.

Name and chemical formula	*S.G.*	*Unit cell*	*Ref.*
	1×1		
Synthetic α-MnO_2	$P4_2/mnm$	*a* 4.3983, *c* 2.8730 Å	[1]
Synthetic TiO_2	$P4_2/mnm$	*a* 4.593, *c* 2.959 Å	[2]
Synthetic GeO_2	$P4_2/mnm$	*a* 4.3975, *c* 2.8625 Å	[3]
Synthetic PbO_2	$P4_2/mnm$	*a* 4.9578, *c* 3.3878 Å	[4]
Cassiterite, SnO_2	$P4_2/mnm$	*a* 4.737, *c* 3.185 Å	[5]
Stishovite, SiO_2	$P4_2/mnm$	*a* 4.1790, *c* 2.6649 Å	[3]
	1×2		
Ramsdellite, MnO_2	*Pbnm*	*a* 4.533, *b* 9.27, *c* 2.866 Å	[6]
Synthetic γ-MnO_2	*Pnam*	*a* 9.3229, *b* 4.4533, *c* 2.8482 Å	[7]
Groutite, MnO(OH)	*Pbnm*	*a* 4.560, *b* 10.700, *c* 2.870 Å	[8]
Goethite, FeO(OH)	*Pbnm*	*a* 4.62, *b* 9.95, *c* 3.01 Å	[9]
Diaspore, AlO(OH)	*Pbnm*	*a* 4.4007, *b* 9.4253, *c* 2.8452 Å	[10]
	2×2		
Hollandite, $Ba(Mn^{4+},Mn^{2+})O_{16}$	*I*4/*m*	*a* 9.96, *c* 2.86 Å	[11]
Hollandite, $Ba(Mn^{4+},Mn^{3+},Fe^{3+})(O,OH)_{16}$	*I*2/*m*	*a* 10.026, *b* 2.878, *c* 9.729 Å, β 91.03°	[12]
Cryptomelane, $K(Mn^{4+},Mn^{2+})O_{16}$	*I*2/*m*	*a* 9.79, *b* 2.88, *c* 9.94 Å, β 90.62°	[13]
Cryptomelane, $K(Mn^{4+},Mn^{3+},)(O,OH)_{16}$	*I*2/*m*	*a* 9.956, *b* 2.870, *c* 9.706 Å, β 90.95°	[12]
Coronadite, $Pb(Mn^{4+},V^{3+})O_{16}$	*I*2/*m*	*a* 9.938, *b* 2.868, *c* 9.834 Å, β 90.39°	[14]
Priderite, $K(Ti,Fe^{3+})O_{16}$	*I*4/*m*	*a* 10.139, *c* 2.966 Å	[12]
Akaganéite, FeO(OH)	*I*2/*m*	*a* 10.587, *b* 3.031, *c* 10.515 Å, β 90.03°	[15]
Manjiroite, $(Na,K)(Mn^{4+},Mn^{3+})_8O_{16}$	*I*4/*m*	*a* 9.916, *c* 2.864 Å	[16]
Strontiomelane, $SrMn^{4+}{}_6Mn^{3+}{}_2O_{16}$	$P2_1/n$	*a* 10.00, *b* 5.758, *c* 9.88 Å, β 90.64°	[17]
Ankangite, $Ba(Ti,V)_8O_{16}$	*I*4/*m*	*a* 10.139, *c* 2.961 Å	[18]
Mannardite, $BaTi_6V_2O_{16}\cdot H_2O$	$I4_1/a$	*a* 14.357, *c* 5.908 Å	[19]
Mannardite, $Ba(Ti,V,Cr)_8(O,OH)_{16}$	*I*4/*m*	*a* 10.071, *c* 14.810 Å	[20]
Redledgeite, $BaTi_6Cr_2O_{16}\cdot H_2O$	*I*2/*m*	*a* 10.129, *b* 2.95, *c* 10.135 Å, β 90.05°	[21]
Redledgeite, $BaTi_6(Cr,Fe,V)_2O_{16}$	*I*4/*m*	*a* 10.1500, *c* 2.9520 Å	[22]
Henrymeyerite, $BaFe^{2+}Ti_7O_{16}$	*I*4/*m*	*a* 10.219, *c* 2.963 Å	[23]
Synthetic $(Ba_{0.58}Pb_{0.51})(Ti,Fe^{3+})_8O_{16}$	*I*4/*m*	*a* 10.1124, *c* 2.9714 Å	[24]
Synthetic $Ba(Ti,Al,Ni)_8O_{16}$	*I*4/*m*	*a* 10.039, *c* 2.943 Å	[25]
Synthetic $KAlSi_3O_8$	*I*4/*m*	*a* 9.38, *c* 2.74 Å	[26]
Synthetic $KAlSi_3O_8$	*I*4/*m*	*a* 9.315, *c* 2.723 Å	[27]
Synthetic $KAlSi_3O_8$ (at 4.47 Gpa)	*I*4/*m*	*a* 9.237, *c* 2.706 Å	[27]
Synthetic $(Ca_{0.5}Mg_{0.5})Al_2Si_2O_8$	*I*2/*m*	*a* 9.384, *b* 8.148, *c* 9.258 Å, β 90.47°	[28]
Synthetic $Pb_{0.8}Al_{1.6}Si_{2.4}O_8$	*I*4/*m*	*a* 9.414, *c* 2.750 Å	[29]
	2×3		
Romanechite, $Ba(Mn^{4+},Mn^{3+})_5O_{10}\cdot H_2O$	*C*2/*m*	*a* 13.929, *b* 2.8459, *c* 9.678 Å, β 92.39°	[30]
	2×4		
Synthetic $Rb_{0.25}(Mn^{4+},Mn^{3+})O_2$	*C*2/*m*	*a* 14.191, *b* 2.851, *c* 24.343 Å, β 91.29°	[31]
Synthetic $Na_{0.33}(Mn^{4+},Mn^{3+})O_2\cdot xH_2O$	*C*2/*m*	*a* 14.434, *b* 2.849, *c* 23.976 Å, β 98.18°	[32]
	2×5		
Synthetic $Rb_{0.27}(Mn^{4+},Mn^{3+})O_2$	*A*2/*m*	*a* 15.04, *b* 2.886, *c* 14.64 Å, β 92.4°	[33]
	3×3		
Todorokite, $(Na,Ca)(Mn^{4+},Mg)_6O_{12}\cdot 5H_2O$	*P*2/*m*	*a* 9.769, *b* 2.8512, *c* 9.560 Å, β 94.47°	[34]
	3×4		
Woodruffite, $Zn_{0.2}(Mn^{4+},Mn^{3+})\cdot 0.7H_2O$	*C*2/*m*	*a* 24.810, *b* 2.8503, *c* 9.581 Å, β 93.845°	[35]

References: [1] Baur 1976; [2] Meagher and Lager 1979; [3] Baur and Khan 1971; [4] D'Antonio and Santoro 1980; [5] Baur 1956; [6] Byström 1949; [7] Fong et al. 1994; [8] Dent Glasser and Ingram 1968; [9] Hoppe 1941; [10] Hill 1979; [11] Byström and Byström 1950; [12] Post et al. 1982; [13] Mathieson and Wadsley 1950; [14] Post and Bish 1989; [15] Post et al. 2003c; [16] Nambu and Tanida 1967; [17] Meisser et al. 1999; [18] Shi et al. 1991; [19] Szymański 1986; [20] Bolotina et al. 1992; [21] Gatehouse et al. 1986; [22] Foley et al. 1997; [23] Mitchell et al. 2000; [24] Reguir et al. 2003; [25] Sinclair et al. 1980; [26] Ringwood et al. 1967a; [27] Zhang et al. 1993; [28] Madon et al. 1989; [29] Downs et al. 1995; [30] Turner and Post 1988; [31] Rziha et al. 1996; [32] Xia et al. 2001; [33] Tamada and Yamamoto 1986; [34] Post et al. 2003b; [35] Post et al. 2003a

Table 2. Octahedral distortion index Δ (= 1/6 $\Sigma[(R_i-R)/R]^2$), computed for all independent octahedra in the given type tunnel structures. In column 2, the number between square brackets refers to the number of equivalent octahedra of the same kind within each ribbon.

Structure type	*Octahedron*	Δ ($\times 10^3$)	*Ref.*
1×1 pyrolusite	M1	0.022	[1]
1×2 ramsdellite	M1 [×2]	0.716	[2]
2×2 priderite	M1 [×2]	0.228	[3]
2×3 romanechite	M1 (central in the 3-ribbon)	0.012	[4]
	M2 (external in the 3-ribbon) [×2]	1.520	
	M3 (2-ribbon) [×2]	0.198	
2×4 RUB-7 (synth.)	M1 (external in the 4-ribbon)	6.531	[5]
	M2 (internal in the 4-ribbon)	1.547	
	M3 (internal in the 4-ribbon)	1.627	
	M4 (external in the 4-ribbon)	5.522	
	M5 (2-ribbon)	3.434	
	M6 (2-ribbon)	1.379	
2×5 $Rb_{0.27}MnO_2$ (synth.)	M1 (central in the 5-ribbon)	0.012	[6]
	M2 (mid-position in the 5-ribbon) [×2]	0.840	
	M3 (external in the 5-ribbon) [×2]	8.451	
	M4 (2-ribbon) [×2]	0.459	
3×3 todorokite	M1 (central in the 3-ribbon)	0.010	[7]
	M3 (central in the 3-ribbon)	0.388	
	M2 (external in the 3-ribbon) [×2]	0.539	
	M4 (external in the 3-ribbon) [×2]	0.237	
3×4 woodruffite	M1 (internal in the 4-ribbon) [×2]	0.184	[8]
	M2 (external in the 4-ribbon) [×2]	5.294	
	M3 (external in the 3-ribbon) [×2]	0.849	
	M4 (central in the 3-ribbon)	0.030	

References: [1] Baur 1976; [2] Fong et al. 1994; [3] Sinclair and McLaughlin 1982; [4] Turner and Post 1988; [5] Rziha et al. 1996; [6] Tamada and Yamamoto 1986; [7] Post et al. 2003b; [8] Post et al. 2003a

using IR spectroscopy suggest the constant occurrence of minor water in ramsdellite, which should be concentrated in a well-defined crystallographic site within the tunnel.

In the ideal 2×2 tunnel structure, the basic tunnel site is the inversion center at (0, 0, 0) and a cation placed in this position is coordinated by 4+4 oxygen atoms, four placed at z=½, four at z=−½ , with A–O distances in the range 2.8–3.0 Å, in the disposition of a distorted tetragonal prism. Moreover, four additional oxygens at distances of ca. 3.5 Å, and at the same z level as the tunnel cation, can be considered as non-coordinating capping anions, one for each of the four vertical faces of the prism (Fig. 2). In several compounds, however, the tunnel cation (K^+, Na^+, Ba^{2+}, Pb^{2+}), is displaced away from the central position. This depends on the high "rigidity" of the cavities, in which the two square planes are forced to be separated by a c translation. Therefore, each tunnel cation, as a function of its ionic radius and of the local geometry of the octahedral framework, may shift closer to either of the two bases of the prism, and possibly may complete its coordination with some of the capping anions. In the case of Pb^{2+} this is favored by the occurrence of a lone pair of electrons. Another reason

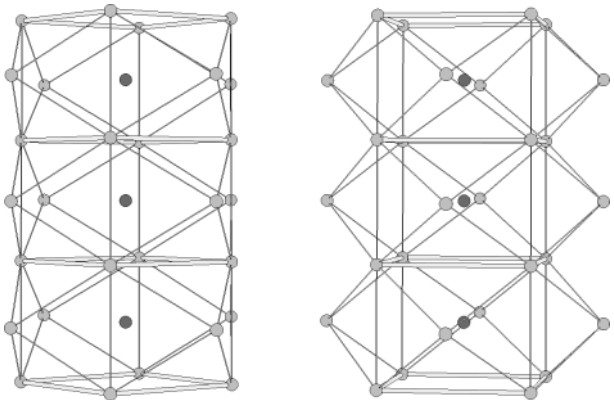

Figure 2. Two perspective views of the tunnel sites in the idealized structure of hollandite-type compound (2×2 tunnels). The tunnel cation is ideally coordinated by 8+4 oxygens (tetracapped tetragonal prism).

for the displacement of the cations from the $(0, 0, 0)$ position is related to the implausibility of placing neighboring tunnel cations on consecutive sites along the *c* axis, which is shorter than 3 Å. This, in some cases, results in several, partly occupied, cation sites along the tunnel axis, which can be described as an incommensurate stacking of tunnel cations with respect to the basic *c* parameter, or alternatively, as superstructures having multiple *c* parameters. Some examples have been mentioned above.

Structures with larger tunnels can incorporate rather more complex sets of cations and/or water molecules. For instance, in romanechite (2×3) the tunnels host two equivalent, IX-coordinated, cation sites, which are occupied by barium. In todorokite (3×3), the tunnels host three independent water molecules, linked by hydrogen bonds between each other and with the oxygen of the octahedral framework. Moreover, a Mg^{2+} cation is placed in the very center of the tunnel, and is octahedrally coordinated by 6 oxygens belonging to the water molecules. In woodruffite (3×4), the tunnels contain four independent water molecules connected to each other and framework oxygens through hydrogen bonding. Moreover, a Zn^{2+} cation is coordinated by 4 oxygens belonging to the water molecules to form a distorted tetrahedron. In synthetic 2×4 and 2×5 compounds, the large cavities are filled by Rb^{+} cations distributed over four partially occupied independent sites and variably coordinated by 8 to 10 oxygen atoms.

Besides pyrolusite, 1×1 tunnels also occur in all structures with larger tunnels where ribbons cross. Some examples of partially occupied 1×1 tunnels have been reported for a Li-bearing todorokite (Duncan et al. 1998) and for woodruffite (Post et al. 2003a). In the latter case, a small Zn occupancy within the 1×1 tunnels is tentatively coupled with a corresponding cation deficiency in the neighbor octahedral sites.

POLYSOMATIC RELATIONSHIPS AMONG COMPOUNDS WITHIN THE PYROLUSITE-"BUSERITE" FAMILY

For these tunnel structures a polysomatic family can be described, that is referred to as the "pyrolusite-'buserite' family," as these structures display the smallest and the largest tunnels so far reported. This family was already sketched by Veblen (1991), who proposed a nomenclature similar to that used for biopyriboles, using P (for pyrolusite) and B (for birnessite). However, unlike biopyriboles, different stacking of P and B can occur along two directions, therefore the symbol for denoting any member of the family becomes quite long in cases of complex

sequences. For instance, the largest tunnel structure so far described, woodruffite, should have the symbol (PBB)×(PBBB). It is more convenient to denote these structures simply by the numeric symbol which defined the openness of the tunnels, which is self-explanatory. In general, it will be a symbol of the kind M×N, with both M and N potentially ranging between 1 and ∞, being M ≤ N (this is purely formal, since of course the structures, e.g., 2×3 and 3×2 are topologically identical between each other, and should not be considered twice). To date, several polysomes have been reported. These have been collected in Table 3, where equidimensional ribbons along the two orthogonal directions are put in the same rows and columns. The values given in Table 3 for each polysome are indicative of the dimensions of a single M×N tunnel, and have been extrapolated from the rough unit cell parameters by subtracting the thickness of the ribbons (octahedral walls). This aims at showing the internal consistency in the lengths and widths of tunnels with the same dimensionality, including the open tunnel of the last column, and the soundness of the polysomatic approach. A schematic drawing of the various tunnel structures is reported in Figure 3.

Table 3. Estimated dimensions of tunnels (in Å) in selected members of the pyrolusite-"buserite" polysomatic family.

1×1 pyrolusite 2.2 × 2.2	[…]	[…]	[…]	[…]	[…]	1×∞ lithiophorite 2.3
	2×2 hollandite 4.7 ×4.7	2×3 romanechite 4.7× 7.3	2×4 RUB-7 4.7 ×9.8	2×5 $Rb_{0.27}MnO_2$ 4.9 × 12.5	[…]	2×∞ birnessite 4.7
		3×3 todorokite 7.3×7.3	3×4 woodruffite 7.2×9.9	[…]	[…]	3×∞ 'buserite' 7.4

Polysomes with infinite ribbons

In the last column of Table 3 some additional minerals have been included that correspond to those M×N polysomes in which N=∞, although these structures, being formed by infinite ribbons (or in other words by octahedral layers) do not have closed tunnels. So far, 1×∞ (lithiophorite), 2×∞ (birnessite), and 3×∞ ('buserite') polysomes are known to occur. The idealized chemical formula of lithiophorite may be written as $(LiAl_2)(Mn^{4+}{}_2Mn^{3+})O_6(OH)_6$; its crystal structure, which was determined by Wadsley (1952) and then refined by Pauling and Kamb (1982) and by Post and Appleman (1994), consist of regularly alternating $(LiAl_2)$ and $(Mn^{4+}{}_2Mn^{3+})$ octahedral layers linked by hydrogen bonds. The distance between neighboring layers is ca. 4.7 Å. Birnessite, a manganese oxide mineral originally described from Scotland with formula $(Na,Ca)Mn_7O_{14}{\cdot}2.8H_2O$ (Jones and Milne 1956), is poorly characterized due to its small crystal dimensions and disordered nature. However, synthetic birnessite is amenable to crystal structure solution (Post and Veblen 1990) and has been determined to be a phyllomanganate in which Mn^{4+}-centered octahedral layers are interleaved with cations (Na, Ca, Mg) and water molecules, with charge balance achieved by Mn^{4+}-Mn^{3+} substitution. The distance between neighbor layers is *ca*. 7.1 Å. "Buserite" is not a valid mineral species, although the name has been extensively used in reference to a disordered phyllomanganate with a dominant 10 Å distance between octahedral layers. Such compounds have been synthesized (Kuma et al. 1994) in which the interlayer cations are Na^+, Mg^{2+}, Ca^{2+}. Typically, "buserite" is obtained as intermediate product during the synthesis of birnessite (e.g., Post 1999; Feng et al. 2004).

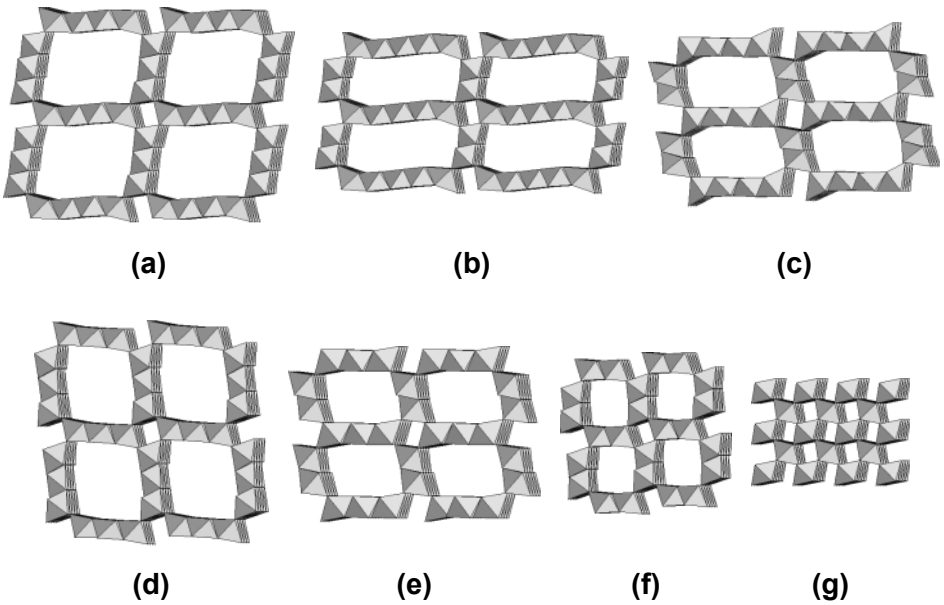

Figure 3. Tunnel structures: (a) woodruffite, 3×4; (b) $Rb_{0.27}MnO_2$ (synthetic), 2×5; (c) RUB-7 (synthetic), 2×4; (d) todorokite, 3×3; (e) romanechite, 2×3; (f) hollandite, 2×2; (g) pyrolusite, 1×1.

True 1×2 polysome

Historically, ramsdellite has been considered a 1×2 tunnel structure and included together with other members of the tunnel oxides, but in strict polysomatic terms this is incorrect. The common feature in tunnel oxides is the occurrence of two sets of ribbons formed by edge-sharing octahedral chains with dimensions ranging from 1 to ∞ that develop in orthogonal directions. This is not the case for ramsdellite where the ribbons (with width corresponding to two octahedral chains) are parallel. Confusingly, in ramsdellite the notation "1×2" refers to the opening of the tunnels but not to the width of the ribbons. Consequently 1×1 tunnels found in all other members of the polysomatic family are absent (Fig. 4). The notation "1×2," whenever referred to the polysomatic description and not to the tunnels, denotes a different structure, which has not been yet reported for any mineral although it has been recognized as local domain within nsutite by HRTEM (Fig. 5).

APPLICATIONS

The technological importance of tunnel oxides arises from three features:

1. Tunnel oxides are very common in nature. A potentially important resource is provided by those manganese oxides that occur in large deposits on the ocean floor and products of mid-ocean ridges (Menard and Shipek 1958).
2. The open structure of tunnel oxides makes them possibly important as cation exchange materials for the sorption of heavy metals. In synthetic analogues these properties may be tailored through controlling the tunnel dimensions.
3. These minerals typically occur as very fine scale aggregates and as coatings with large surface areas that may further enhances their exchange capacity.

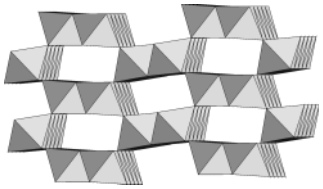

Figure 4. Structural scheme of ramsdellite: it has 1×2 tunnels, but does not correspond to the 1×2 polysome.

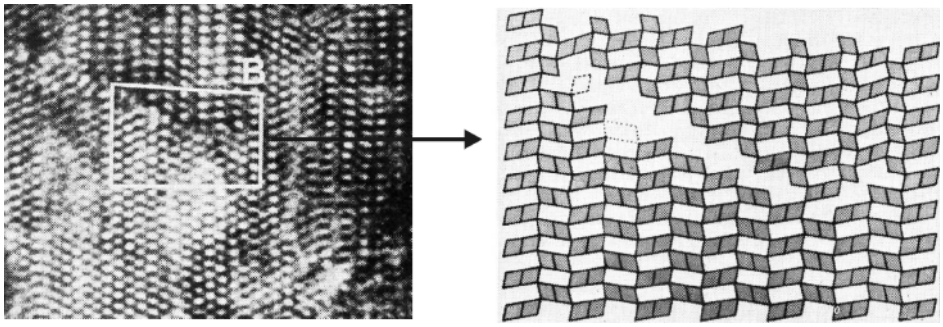

Figure 5. On the left side, HRTEM photo of nsutite from Piedra Negras, Mexico, showing several defects. The structural arrangement of ribbons in the region within the B box is sketched on the right side; the upper right region corresponds to the "true" 1×2 polysome, whereas the lower left region corresponds to ramsdellite, the "false" 1×2 polysome [Used by permission of Nature Publishing Group, from Turner and Buseck (1983), Nature, Vol. 304, Fig. 4, p. 145].

These three features are common with zeolites, although the first is perhaps limited due to the difficulty of mining deep ocean deposits. Generally however, technological applications do not require comprehensive characterization of fine-grained and poorly crystalline phases, as their useful industrial properties are apparently independent of crystal chemistry, at least as the first approximation. According to Post (1999), the most common manganese oxide minerals in soils are lithiophorite, hollandite, and birnessite.

Already manganese tunnel oxides are exploited due to their microporous features. Specifically, tunnel oxides are often referred to as Octahedral Molecular Sieves (OMS), a terminology that mirrors the acronym ZSM that is applied to zeolite-like molecular sieves based on a tetrahedral framework. The wide range of applications of tunnel oxides include:

i. The inclusion in a high level radioactive waste of a compound with composition $BaAl_2Ti_6O_{16}$ and structurally related to hollandite (2×2) called SYNROC (Ringwood et al. 1979) specifically for the immobilisation of radioactive cesium.

ii. Amelioration of pollution using manganese oxides that may act as natural sinks for heavy metals in contaminated waters from mines and other industrial activities (Whitney 1975; Lind and Hem 1993). For instance, the capability of cryptomelane to sorb cations such as Co^{2+}, Zn^{2+}, and Cd^{2+} has been discussed by Ghoneimy (1997) and Randall et al. (1998).

iii. Photocatalytic oxidation (e.g., birnessite, todorokite) for environmental remediation and modifying soil chemistry (Oscarson et al. 1981; Shen et al. 1993).

iv. Ion exchange media in a variety of uses. Synthetic todorokite (3×3) obtained in a two-step procedure after synthetic birnessite ($2 \times \infty$), shows significant cation exchange properties similar to zeolites (Golden et al. 1986). This may prove to be true for other oxides with large tunnels (3×4, 2×5).

Finally, tunnel oxides are of considerable scientific interest in pure and applied geosciences. As noted earlier, feldspars assume hollandite-type structures at very high pressure and may represent one of the major phases in the Earth's mantle.

ACKNOWLEDGMENTS

Marco Bellezza assisted with the art work. The paper benefited from reviews by Giovanni Ferraris, Sergey Krivovichev, Emil Mackovicky, and Tim White.

REFERENCES

Baur WH (1956) Über der Verfeinerung der Kristallstrukturbestimmung einiger Vertreter des Rutiltyps: TiO_2, SnO_2, GeO_2 und MgF_2. Acta Crystallogr 9:515-520

Baur WH (1976) Rutile-type compounds. V. Refinement of MnO_2 and MgF_2. Acta Crystallogr B32:2200-2204

Baur WH, Khan AA (1971) Rutile-type compounds. IV. SiO_2, GeO_2 and a comparison with other rutile-type structures. Acta Crystallogr B27:2133-2139

Bayer G, Hoffman W (1966) Complex alkali titanium oxides $A_xB_yTi_{8-y}O_{16}$ of the α-MnO_2 structure-type. Am Mineral 51:511-516

Bolotina NB, Dmitrieva MT, Rastsvetaeva RK (1992) Modulated structures of a new natural representative of the hollandite series. Sov Phys Crystallogr 37:311-315

Burns RG, Burns VM, Stockman HW (1983) A review of the todorokite-buserite problem: implications to the mineralogy of marine manganese nodules. Am Mineral 68:972-980

Burns RG, Burns VM, Stockman HW (1985) The todorokite-buserite problem: further considerations. Am Mineral 70:205-208

Byström A, Byström AM (1950) The crystal structure of hollandite, the related manganese oxide minerals and α-MnO_2. Acta Crystallogr 3:146-154

Byström A, Byström AM (1951) The positions of the barium atoms in hollandite. Acta Crystallogr 4:469

Byström AM (1949) The crystal structure of ramsdellite, an orthorhombic modification of MnO_2. Acta Chem Scand 3:163-173

Chukhrov FV, Gorshkov AI, Dmitriyeva MT, Sivtsov AV (1983) Crystallochemistry of romanechite. Int Geol Rev 25:517-525

Chukhrov FV, Gorshkov AI, Drits VA, Dikov YP (1985) Structural varieties of todorokite. Int Geol Rev 27: 1481-1491

Chukhrov FV, Gorshkov AI, Sivtsov AV, Berezovskaya VV (1980) Structural varieties of todorokite. Int Geol Rev 22:75-83

D'Antonio P, Santoro A (1980) Powder neutron diffraction study of chemically prepared β-lead dioxide. Acta Crystallogr B36:2394-2397

Dachs H (1963) Neutronen- und Röntgenuntersuchungen an Manganit, MnOOH. Z Kristallogr 118:303-326

De Wolff PM (1959) Interpretation of some γ-MnO_2 diffraction patterns. Acta Crystallogr 12:341-345

Dent Glasser LS, Ingram L (1968) Refinement of the crystal structure of groutite, α–MnOOH. Acta Crystallogr B24:1233-1236

Downs RT, Hazen RM, Finger LW (1995) Crystal chemistry of lead aluminosilicate hollandite: a new high-pressure synthetic phase with octahedral Si. Am Mineral 80:937-940

Duncan MJ, Leroux F, Corbett JM, Nazar LF (1998) Todorokites as a Li insertion cathode. J Electrochem Soc 145:3746-3757

Feng XH, Liu F, Tan WF, Liu XW (2004) Synthesis of birnessite from the oxidation of Mn^{2+} by O_2 in alkali medium: effects of synthesis conditions. Clays Clay Mineral 52:240-250

Foley JA, Hughes JM, Drexler JW (1997) Redledgeite, $Ba_x([Cr,Fe,V]^{3+}_{2x}Ti_{8-2x})O_{16}$, the *I*4/*m* structure and elucidation of the sequence of tunnel Ba cations. Can Mineral 35:1531-1534

Foley S, Hoefer H, Brey G (1994) High-pressure synthesis of priderite and members of the lindsleyite-mathiasite and hawthorneite-yimengite series. Contrib Mineral Petrol 117:164-174.

Fong C, Kennedy BJ, Elcombe MM (1994) A powder neutron diffraction study of λ and γ manganese dioxide and of $LiMn_2O_4$. Z Kristallogr 209:941-945

Fritsch S, Post JE, Navrotsky A (1997) Energetics of low-temperature polymorphs of manganese dioxide and oxyhydroxide. Geochim Cosmochim Acta 61:2613-2616

Frondel C (1953) New manganese oxides: hydrohausmannite and woodruffite. Am Mineral 38:761-769

Gaines RV, Skinner HCW, Foord EE, Mason B, Rosenzweig A (1997) Dana's New Mineralogy, 8th ed. Wiley, New York

Gatehouse BM, Jones GC, Pring A, Symes RF (1986) The chemistry and structure of redledgeite. Mineral Mag 50:709-715
Ghoneimy HF (1997) Adsorption of Co^{2+} and Zn^{2+} on cryptomelane-type hydrous manganese dioxide. J Radioanal Nucl Chem 223:61-65
Giovanoli R (1985) A review of the todorokite-buserite problem: implications to the mineralogy of marine manganese nodules: discussion. Am Mineral 70:202-204
Golden DC, Chen CC, Dixon JB (1986) Synthesis of todorokite. Science 231:717-719
Hill R (1979) Crystal structure refinement and electron density distribution in diaspore. Phys Chem Minerals 5:179-200
Hoppe W (1941) Über die Kristallstruktur von α-AlOOH (Diaspor) und α-FeOOH (Nadeleisenerz). Z Kristallogr 103:73-89
Jones LHP, Milne AA (1956) Birnessite, a new manganese oxide mineral from Aberdeenshire, Scotland. Mineral Mag 31:283-288
Kikuchi T, Yoshino T, Miura H (1994) Orthorhombic distortion in pyrolusites. 16th Gen Meet Int Mineral Ass, Pisa, 4-9 Sep, abstr, 203-204
Kudo H, Miura H, Hariya Y (1990) Tetragonal-monoclinic transformation of cryptomelane at high temperature. Mineral J 15:50-63
Kuma K, Usui A, Paplawsky W, Gedulin B, Arrhenius G (1994) Crystal structures of synthetic 7 Å and 10 Å manganates substituted by mono- and divalent cations. Mineral Mag 58:425-447
Lind CJ, Hem JD (1993) Manganese minerals and associated fine particulates in the streambed of Pinal Creek, Arizona, U.S.A.: a mining-related acid drainage problem. Appl Geochem 8:67-80
Liu ZH, Ooi K (2003) Preparation and alkali-metal ion extraction/insertion reactions with nanofibrous manganese oxide having 2×4 tunnel structure. Chem Mater 15:3696-3703
Madon M, Castex J, Peyronneau J (1989) A new aluminosilicate high-pressure phase as a possible host of calcium and aluminum in the lower mantle. Nature 342:422-425
Mathieson AM, Wadsley AD (1950) The crystal structure of cryptomelane. Am Mineral 35:99-101
McCusker LB (2005) IUPAC nomenclature for ordered microporous and mesoporous materials and its application to non-zeolite microporous mineral phases. Rev Mineral Geochem 57:1-16
Meagher EP, Lager GA (1979) Polyhedral thermal expansion in the TiO_2 polymorphs: refinement of the crystal structures of rutile and brookite at high temperature. Can Mineral 17:77-85
Meisser N, Perseil EA, Brugger J, Chiappero PJ (1999) Strontiomelane, $SrMn^{4+}{}_6Mn^{3+}{}_2O_{16}$, a new mineral species of the cryptomelane group from St. Marcel-Praborna, Aosta Valley, Italy. Can Mineral 37:673-678
Menard HW, Shipek CJ (1958) Surface concentrations of manganese nodules. Nature 182:1156-1158
Mitchell RH, Yakovenchuk VN, Chakhmouradian AR, Burns PC, Pakhomovsky YA (2000) Henrymeyerite, a new hollandite-type Ba-Fe titanate from the Kovdor Complex, Russia. Can Mineral 38:617-626
Miura H, Kudou H, Choi JH, Hariya Y (1990) The crystal structure of ramsdellite from Pirika Mine. J Fac Sci Hokkaido Univ, Ser 4, Geol Mineral 22:611-617
Nambu M, Tanida K (1967) Manjiroite, a new manganese dioxide mineral, from Kohare Mine, Iwate prefecture, Japan. J Japan Ass Mineral Petrol Econ Geol 58:39-54
Oscarson DW, Huang PM, Liaw WK (1981) The role of manganese in the oxidation of arsenite by freshwater lake sediments. Clays Clay Minerals 29:219-225
Pauling L, Kamb B (1982) The crystal structure of lithiophorite. Am Mineral 67:817-821
Post JE (1999) Manganese oxide minerals: crystal structures and economic and environmental significance. Proc Nat Acad Sci USA 96:3447-3454
Post JE, Appleman DE (1994) Crystal structure refinement of lithiophorite. Am Mineral 79:370-374
Post JE, Bish DL (1988) Rietveld refinement of the todorokite structure. Am Mineral 73:861-869
Post JE, Bish DL (1989) Rietveld refinement of the coronadite structure. Am Mineral 74:913-917
Post JE, Heaney PJ (2004) Neutron and synchrotron X-ray diffraction study of the structures and dehydration behaviors of ramsdellite and "groutellite." Am Mineral 89:969-975
Post JE, Heaney PJ, Cahill CL, Finger LW (2003a) Woodruffite: a new Mn oxide structure with 3×4 tunnels. Am Mineral 88:1697-1702
Post JE, Heaney PJ, Hanson J (2003b) Synchrotron X-ray diffraction study of the structure and dehydration behavior of todorokite. Am Mineral 88:142-150
Post JE, Heaney PJ, Hanson JC (2001) Temperature-resolved synchrotron X-ray diffraction study of ramsdellite and groutite. Geol Soc Am Ann Meet, Boston, abstr, 33:362-363
Post JE, Heaney PJ, Von Dreele RB, Hanson JC (2003c) Neutron and temperature-resolved synchrotron X-ray powder diffraction study of akaganéite. Am Mineral 88:782-788
Post JE, Veblen DR (1990) Crystal structure determination of synthetic sodium, magnesium, and potassium birnessite using TEM and the Rietveld method. Am Mineral 75:477-489

Post JE, Von Dreele RB, Buseck PR (1982) Symmetry and cation displacements in hollandites: structure refinements of hollandite, cryptomelane and priderite. Acta Crystallogr B38:1056-1065
Potter RM, Rossman GR (1979) The tetravalent manganese oxides: identification, hydration, and structural relationships by infrared spectroscopy. Am Mineral 64:1199-1218
Randall SR, Sherman DM, Ragnarsdottir KV (1998) An extended X-ray absorption fine structure spectroscopy investigation of cadmium sorption on cryptomelane (KMn_8O_{16}). Chem Geol 151:95-106
Reguir EP, Chakhmouradian AR, Mitchell RH (2003) Pb-bearing hollandite-type titanates: a first natural occurrence and reconnaissance synthesis study. Mineral Mag 67:957-965
Ringwood AE, Kesson SE, Ware NG, Hibberson W, Major A (1979) Immobilization of high level nuclear reactor wastes in SYNROC. Nature 278: 219-223
Ringwood AE, Reid AF, Wadsley AD (1967a) High pressure $KAlSi_3O_8$, an aluminosilicate with sixfold coordination. Acta Crystallogr 23:1093-1095
Ringwood AE, Reid AF, Wadsley AD (1967b) High pressure transformation of alkali aluminosilicates and aluminogermanates. Earth Planet Sci Letters 3:38-40
Rziha T, Gies H, Rius J (1996) RUB-7, a new synthetic manganese oxide structure type with a 2×4 tunnel. Eur J Mineral 8:675-686
Shen X, Ding Y, Liu J, Laubernds K, Zerger RP, Polverejan M, Son YC, Aindow M, Suib SL (2004) Synthesis, characterization and catalytic applications of manganese oxide octahedral molecular sieve (OMS) nanowires with a 2×3 tunnel structure. Chem Mater 16:5327-5335
Shen YF, Zerger RP, DeGuzmaz RN, Suib SL, McCurdy L, Potter DI, O'Young CL (1993) Manganese oxide octahedral molecular sieves: preparation, characterization, and applications. Science 260:511-515
Shi N, Ma Z, Liu W (1991) Crystal structure determination of ankangite with one-dimensional incommensurate modulation. Acta Petrol Mineral 10:233-245 (in Chinese)
Sinclair W, McLaughlin GM (1982) Structure refinement of priderite. Acta Crystallogr B38:245-256
Sinclair W, McLaughlin GM, Ringwood AE (1980) The structure and chemistry of a barium titanate hollandite-type phase. Acta Crystallogr 36:2913-2918
Strunz H, Nickel EH (2001) Strunz Mineralogical Tables, 9th ed. Schweizertbart'sche, Stuttgart
Szymański JT (1986) The crystal structure of mannardite, a new hydrated cryptomelane-group (hollandite) mineral with a doubled short axis. Can Mineral 24:67-78
Tamada O, Yamamoto N (1986) The crystal structure of a new manganese dioxide ($Rb_{0.27}MnO_2$) with a giant tunnel. Mineral J 13:130-140
Turner S, Buseck PR (1979) Manganese oxide tunnel structures and their intergrowths. Science 203:456-458
Turner S, Buseck PR (1981) Todorokites: a new family of naturally occurring manganese oxides. Science 212: 1024-1027
Turner S, Buseck PR (1983) Defects in nsutite (γ-MnO_2) and dry-cell battery efficiency. Nature 304:143-146
Turner S, Post JE (1988) Refinement of the substructure and superstructure of romanechite. Am Mineral 73: 1155-1161
Veblen DR (1991) Polysomatism and polysomatic series: a review and applications. Am Mineral 76:801-826
Vicat J, Fanchon E, Strobel P, Qui DT (1986) The structure of $K_{1.33}Mn_8O_{16}$ and cation ordering in hollandite-type structures. Acta Crystallogr B42:162-167
Wadsley AD (1952) The structure of lithiophorite, $(Al,Li)MnO_2(OH)_2$. Acta Crystallogr 5:676-680
Wadsley AD (1953) The crystal structure of psilomelane, $(Ba,H_2O)Mn_5O_{10}$. Acta Crystallogr 6:433-438
Whitney PR (1975) Relationship of manganese-iron oxides and associated heavy metals to grain size in stream sediments. J Geochem Expl 4:251-263
Wu XJ, Li FH (1990) Electron microscopy study of incommensurately modulated structure of ankangite. Acta Crystallogr 46:111-117
Xia GG, Tong W, Tolentino EN, Duan NG, Brock SL, Wang JY, Suib SL, Ressler T (2001) Synthesis and characterization of nanofibrous sodium manganese oxide with a 2×4 tunnel structure. Chem Mater 13: 1585-1592
Yamada H, Matsui Y, Ito E (1984) Crystal-chemical characterization of $KAlSi_3O_8$ with the hollandite structure. Mineral J 12:29.34
Yoshino T, Miura H, Hariya Y (1992) Crystal structure of orthorhombic pyrolusite. 29th Int Geol Congr, Kyoto, Aug 24 - Sep 3, abstr, 216
Yoshino T, Miura H, Hariya Y (1993) Crystal structure of orthorhombic pyrolusite from Imini Mine, Marrakesh, Morocco. *In*: Mineral resources symposia. S Ishihara, T Urabe, H Ohmoto (eds) Society of Resource Geologists of Japan, Tokyo, p. 62-65
Zhang J, Burnham CW (1994) Hollandite-type phase: geometric consideration of unit-cell size and symmetry. Am Mineral 79:168-174
Zhang J, Ko J, Hazen RM, Prewitt CT (1993) High-pressure crystal chemistry of $KAlSi_3O_8$ hollandite. Am Mineral 78:493-499
Zwicker WK, Meijer WOJG, Jaffe HW (1962) Nsutite, a widespread manganese oxide mineral. Am Mineral 47:246-266